



Submicron aerosols at thirteen diversified sites in China

J. F. Peng et al.

This discussion paper is/has been under review for the journal Atmospheric Chemistry and Physics (ACP). Please refer to the corresponding final paper in ACP if available.

# Submicron aerosols at thirteen diversified sites in China: size distribution, new particle formation and corresponding contribution to cloud condensation nuclei production

J. F. Peng<sup>1</sup>, M. Hu<sup>1</sup>, Z. B. Wang<sup>1</sup>, X. F. Huang<sup>2</sup>, P. Kumar<sup>3,4</sup>, Z. J. Wu<sup>1</sup>, D. L. Yue<sup>1</sup>, S. Guo<sup>1</sup>, D. J. Shang<sup>1</sup>, Z. Zheng<sup>1</sup>, and L. Y. He<sup>2</sup>

<sup>1</sup>State Key Joint Laboratory of Environmental Simulation and Pollution Control, College of Environmental Sciences and Engineering, Peking University, Beijing 100871, China

<sup>2</sup>Key Laboratory for Urban Habitat Environmental Science and Technology, School of Environment and Energy, Peking University Shenzhen Graduate School, Shenzhen 518055, China

<sup>3</sup>Department of Civil and Environmental Engineering, Faculty of Engineering and Physical Sciences (FEPS), University of Surrey, Guildford GU2 7XH, UK

<sup>4</sup>Environmental Flow (EnFlo) Research Centre, FEPS, University of Surrey, Guildford GU2 7XH, UK

Title Page

Abstract

Introduction

Conclusions

References

Tables

Figures



Back

Close

Full Screen / Esc

Printer-friendly Version

Interactive Discussion



Received: 21 May 2014 – Accepted: 24 May 2014 – Published: 11 June 2014

Correspondence to: M. Hu (minhu@pku.edu.cn)

Published by Copernicus Publications on behalf of the European Geosciences Union.

**ACPD**

14, 15149–15189, 2014

**Submicron aerosols  
at thirteen diversified  
sites in China**

J. F. Peng et al.

Title Page

Abstract

Introduction

Conclusions

References

Tables

Figures



Back

Close

Full Screen / Esc

Printer-friendly Version

Interactive Discussion



## Abstract

Understanding the particle number size distributions in diversified atmospheric environments is important in order to design mitigation strategies related to submicron particles and their effect on regional air quality, haze and human health. In this study, we conducted 15 different field measurement campaigns, each one-month long, between 2007 and 2011 at 13 individual sites in China. These were 5 urban sites, 4 regional sites, 3 coastal/background sites and one ship cruise measurement along eastern coastline of China. Size resolved particles were measured in the 15–600 nm size range. The median particle number concentrations (PNC) were found to vary in the range of  $1.1\text{--}2.2 \times 10^4 \text{ cm}^{-3}$  at urban sites,  $0.8\text{--}1.5 \times 10^4 \text{ cm}^{-3}$  at regional sites,  $0.4\text{--}0.6 \times 10^4 \text{ cm}^{-3}$  at coastal/background sites, and  $0.5 \times 10^4 \text{ cm}^{-3}$  during cruise measurements. Peak diameters at each of these sites varied greatly from 24 nm to 115 nm. Particles in the 15–25 nm (nucleation mode), 25–100 nm (Aitken mode) and 100–600 nm (accumulation mode) range showed different characteristics at each of the studied sites, indicating the features of primary emissions and secondary formation in these diversified atmospheric environments. Diurnal variations show a build-up of accumulation mode particles belt at regional sites, suggesting the contribution of regional secondary aerosol pollution. Frequencies of new particle formation (NPF) events were much higher at urban and regional sites than at coastal sites and cruise measurement. The average growth rates (GRs) of nucleation mode particles were  $8.0\text{--}10.9 \text{ nm h}^{-1}$  at urban sites,  $7.4\text{--}13.6 \text{ nm h}^{-1}$  at regional sites and  $2.8\text{--}7.5 \text{ nm h}^{-1}$  at both coastal and cruise measurement sites. The high gaseous precursors and strong oxidation at urban and regional sites not only favored the formation of particles, but also accelerated the growth rate of the nucleation mode particles. No significant difference in condensation sink (CS) during NPF days were observed among different site types, suggesting that the NPF events in background area were more influenced by the pollutant transport. In addition, average contributions of NPF events to potential cloud condensation nuclei (CCN) at 0.2 % super-saturation in the afternoon of all sampling days were calculated

### Submicron aerosols at thirteen diversified sites in China

J. F. Peng et al.

Title Page

Abstract

Introduction

Conclusions

References

Tables

Figures



Back

Close

Full Screen / Esc

Printer-friendly Version

Interactive Discussion



as 11 % and 6 % at urban sites and regional sites, respectively. On the other hand, NPF events at coastal and cruise measurement sites had little impact on potential production of CCN. This study provides a large dataset of aerosol size distribution in diversified atmosphere of China, improving our general understanding of emission, secondary formation, new particles formation and corresponding CCN activity of submicron aerosols in Chinese environments.

## 1 Introduction

Atmospheric particles play an important role in the degradation of visibility and changing the balance of global radiative forcing (Dusek, 2006; IPCC, 2010), besides showing adverse impacts on human health (Heal et al., 2012). Size of atmospheric particles, ranging from a few nanometers up to hundreds of micrometers, is a key factor for evaluating environmental effects of particles (Buseck and Adachi, 2008; Kumar et al., 2014). For example, particle diameter is considered to be more important than chemical composition for cloud-nucleating ability (Dusek, 2006). Smaller particles may have greater potential of health impacts compared with their larger counterparts (WHO, 2013). Particles smaller than 100 nm in diameter (which are sum of nucleation and Aitken mode particles) have deeper deposition in human body and are able to induce more intense oxidative stress in cells (Nel et al., 2006). Accumulation mode particles (those in the 100–1000 nm size range), on the other hand, have high light extinction efficiency and can explain degradation of visibility in severe air pollution event to a great extent (See et al., 2006). Meanwhile, particle size distribution offers information on type, origin, and atmospheric transformation of the particles (Buseck and Adachi, 2008; Harrison et al., 2011). Therefore, the knowledge of size distributions of submicron particles, including their temporal and spatial variability, is crucial in characterizing human exposure, estimating climate effects, and designing monitoring strategies for both developed and developing countries (Kumar et al., 2014).

Measurements of particle number distribution (PND) have been extensively conducted in many European and US sites in the past two decades (A. Asmi et al., 2011; Bigi and Ghermandi, 2011; Borsos et al., 2012; Kumar et al., 2010; Wehner and Wiedensohler, 2003) but at a much lesser extent in developing countries (Monkko-

5 nenen et al., 2005; Wu et al., 2008; Kumar et al., 2011; Wang et al., 2013a). Temporal and spatial variation of PND in these developed countries has been widely recognized (A. Asmi et al., 2011). Whilst these particles arise from a number of non-vehicle exhaust sources (Kumar et al., 2013b), primary emission from road vehicles is thought to be a main source of particle number concentration (PNC) in urban areas (Kumar et al., 2010).

The new particle formation (NPF), associated with a rapid burst in nucleation mode particles, results in an increase of CCN number after growth (Wiedensohler et al., 2009). The NPF events were observed in many atmospheric environments in the world, especially in relatively clean atmosphere (Kulmala et al., 2013). However, the obser-

15 vations of NPF events are still rare in developing countries. Though the first study on NPF events during polluted episodes was conducted in the megacity of Beijing (Wehner et al., 2004; Wu et al., 2007), but the occurrence of NPF events is yet reported only at a few sites in China (Du et al., 2012; Liu et al., 2008; Wang et al., 2013b; Wehner et al., 2004; Wiedensohler et al., 2009). Although it is a common interest that regional NPF

20 events are a main source of atmospheric CCN production (Kuang et al., 2009), most of the estimation on the contribution of NPF events to CCN concentration till date are only based on model simulations using regional/global scale models with extra NPF mode (Merikanto et al., 2009; Yu et al., 2012). The only few measurement studies that attempted to quantify the strength of this nucleation process merely calculated the en-

25 hancement of CCN concentration along with NPF events (Yue et al., 2011; Kerminen et al., 2012; Kuang et al., 2009; E. Asmi et al., 2011). Modelling results presented so far are likely to be greatly influenced by factors such as change of boundary layer as well as primary emissions. More measurements and new measurement-based approaches

## Submicron aerosols at thirteen diversified sites in China

J. F. Peng et al.

[Title Page](#)[Abstract](#)[Introduction](#)[Conclusions](#)[References](#)[Tables](#)[Figures](#)[Back](#)[Close](#)[Full Screen / Esc](#)[Printer-friendly Version](#)[Interactive Discussion](#)

**Submicron aerosols  
at thirteen diversified  
sites in China**

J. F. Peng et al.

[Title Page](#)[Abstract](#)[Introduction](#)[Conclusions](#)[References](#)[Tables](#)[Figures](#)[Back](#)[Close](#)[Full Screen / Esc](#)[Printer-friendly Version](#)[Interactive Discussion](#)

are therefore needed to estimate the contribution of NPF to corresponding CCN concentration in diversified environments.

China has been experiencing unprecedented modernization and urbanization process since 1980s. The rapid industrial revolution has intensively occurred in China during the past 30 years, providing both the chance to become “the world factory” and the challenge of severe air pollution problem. The aerosol pollution in recent years at both local and regional scale has attracted great attention, as it results in the heavy smog or haze episodes and might lead to potential health effects (Xu et al., 2013). The aerosol pollution characterizes regional property in major economic developed regions with megacity or city clusters, for instance, Bohai Sea Rim Region, Yangtze River Delta and Pearl River Delta. To understand the feature of aerosol pollution in these regions requires multi-site measurements within each pollution region.

In this study, we have therefore conducted PND measurements at 13 different sites in China in order to provide comprehensive understanding of the effects of primary emissions, regional pollutants transportation and new particle formation on PNDs. These sites are classified into four main categories – urban, regional, coastal and ship cruising – representing the typical atmospheric environments in China. Unique features of each of these sites, along with the particle number and size distributions measured, are discussed in Sects. 2 and 3, respectively. Special focus is given to the NPF events and their contribution to CCN concentration at each of the thirteen sites.

## 2 Methodology

### 2.1 Sites description

A total of 15 field measurement campaigns of PNDs were conducted at 13 different sites between 2007 and 2011. These sites were broadly classified in the following four types of atmospheric environment categories (see Table 1). These included five urban sites, four regional sites, three coastal/background sites and one ship cruise

measurement along Eastern coastal China. As shown in Fig. 1, most of these sites were situated in the most developed and largest city cluster regions in China.

### 2.1.1 Urban sites

The first urban site, Guangzhou ( $GZ_u$ ;  $23.13^\circ$  N,  $113.26^\circ$  E) was located on the roof of the Guangdong Provincial Environmental Monitoring Center in the downtown of Guangzhou, at a height of about 50 m above street level (Yue et al., 2013). This site is representative of a typical ambient conditions in Guangzhou urban areas (Zhang et al., 2008).

The second urban site, Shanghai ( $SH_u$ ;  $21.53^\circ$  E,  $31.23^\circ$  N), was a megacity located in the east of the Yangtze River Delta region of China, facing the East China Sea.  $SH_u$  was located on the roof of a 6-floor building of Shanghai Pudong Environmental Monitoring Station. The surroundings of this site were mainly residential and business buildings (Huang et al., 2012).

The third urban site, Urumchi ( $UR_u$ ;  $87.58^\circ$  N,  $43.83^\circ$  E), was located on roof of the Urumchi Environmental Monitoring Center in the downtown of Urumchi city. Urumchi city is the capital of Xinjiang Uyghur Autonomous Region, with the biggest desert in China to the north and mountains to the south. Sampling inlet at  $UR_u$  site was located at  $\sim 20$  m above the street level. The surroundings of this site were mainly residential and business buildings. There was one main road 200 m away to the west and another 400 m away to the east.

The fourth urban site, Wuxi ( $WX_u$ ;  $31.56^\circ$  N,  $120.29^\circ$  E), was located on the roof of a five-floor building in the center of Wuxi City. This site was surrounded by the residential buildings. No obvious stationary sources existed nearby and the nearest main road was about 300 m away to the east. Sampling inlet was at  $\sim 15$  m above the ground level.

The fifth urban site, Jinhua ( $JH_u$ ;  $29.1^\circ$  N,  $119.69^\circ$  E), was located on the roof of the Jindong Environmental Building in the east part of the city of Jinhua. Sampling inlet was at  $\sim 25$  m above the street level. There was no industry source nearby and the nearest

## Submicron aerosols at thirteen diversified sites in China

J. F. Peng et al.

Title Page

Abstract

Introduction

Conclusions

References

Tables

Figures



Back

Close

Full Screen / Esc

Printer-friendly Version

Interactive Discussion



main road was located  $\sim 300$  m away to the west. As the wind direction is always from northeast during the measurements (October), the influence of this main road on our site can be ignored.

### 2.1.2 Regional sites

5 The first regional site, Heshan ( $HS_r$ ;  $22.71^\circ$  N,  $112.93^\circ$  E), was an urban outflow site of Guangzhou megacity in central Pearl River Delta (PRD), with a distance from Guangzhou downtown 50 km. It was located on the top of a small hill (40 m), about 7 km away from Heshan downtown areas, and was far from strong industrial sources. The surrounding areas of the site were dominated by farmlands and forests. Biomass  
10 burning events were observed occasionally in the farmlands. This site can be well representative of the air pollution outflow from the polluted central PRD urban areas (Gong et al., 2012).

The second regional site, Kaiping ( $KP_r$ ;  $22.33^\circ$  N,  $112.54^\circ$  E), is located  $\sim 120$  km away from the city of Guangzhou to the southwest. Under the influence of the Asian  
15 monsoon, the dominant air mass comes to PRD from the northeast in fall. Hence, the Kaiping site could be assumed to be a downwind receptor site. Instruments were placed on the third floor of the building at the Kaiping supersite ( $\sim 10$  m above the ground level), which is surrounded by shrubs and eucalyptus forest (Wang et al., 2013b). The site is free of any significant local pollution emissions. A detailed geo-  
20 graphic description of this measurement site can be seen elsewhere (Huang et al., 2011).

The third regional site, Jiaxing ( $JX_r$ ;  $30.8^\circ$  N,  $120.8^\circ$  E), was a suburban site between Shanghai and Hangzhou. It was located on the roof of school building in a small town,  
15 m above the ground level and 8 km away from the downtown of Jiaxing city, which  
25 was situated in the middle of Shanghai megacity and Hangzhou, capital of Zhejiang province.

The fourth regional site, Yufa ( $YF_r$ ;  $39.51^\circ$  N,  $116.3^\circ$  E), was about 40 km to the south of Beijing downtown area. This site was located on top of a building ( $\sim 20$  m above

## Submicron aerosols at thirteen diversified sites in China

J. F. Peng et al.

Title Page

Abstract

Introduction

Conclusions

References

Tables

Figures



Back

Close

Full Screen / Esc

Printer-friendly Version

Interactive Discussion





the ground level) at the campus of Huangpu College. There were no industrial sources around this site, except the farm land and a residential area (Guo et al., 2010).

### 2.1.3 Three coastal/background sites

5 The first coastal site, Baguang ( $BG_c$ ;  $22.65^\circ$  N,  $114.54^\circ$  E), was located on the roof of a three-floor building ( $\sim 10$  m a.s.l.) at the seaside in a small peninsula in the southern China, 50 km away from the city of Shenzhen to the east. No stationary source or traffic source was found nearby the site. To the east and south of the site was the South China Sea. This site can well represent the background atmosphere of southern China during autumn.

10 The second coastal site, Wenling ( $WL_c$ ;  $28.40^\circ$  N,  $121.61^\circ$  E), was a coastal/background site. This site was located in a flat ground area in a peninsula in the southeast of China, and was surrounded by only farmland. The sampling inlet was about 4 m above the ground level. The East China Sea was up to 2 km away from the site to the northeast and southeast. The city of Taizhou was about 30 km away to the northwest of the site. Wind direction ranged from north to east during the whole campaign at  $WL_c$  site, resulting in a variety of air masses that can be encountered from modified clean maritime to continental polluted.

15 The third coastal site, Changdao ( $CD_c$ ;  $37.99^\circ$  N,  $120.70^\circ$  E), was located at  $\sim 50$  m above the sea level on a hill in the north coast of an island. This island was located offshore to the east edge of central eastern China and laid between the Jiaodong and the Liaodong Peninsula in the Bohai Sea, called Changdao. The Changdao Island was surrounded by sea on three sides and connected with a larger island by a bridge on the south side. A detailed geographic description of the measurement site is presented in (Hu et al., 2013).

## Submicron aerosols at thirteen diversified sites in China

J. F. Peng et al.

Title Page

Abstract

Introduction

Conclusions

References

Tables

Figures



Back

Close

Full Screen / Esc

Printer-friendly Version

Interactive Discussion



## 2.1.4 Ship cruise measurement

Ship cruise measurement ( $ES_s$ ) was carried out on the “Dong Fang Hong 2”, which is a multi-functional marine research vessel (<http://eweb.ouc.edu.cn/4b/61/c4169a19297/page.htm>). The observatory was located on the 6th floor of the “Dong Fang Hong 2”, which was about 15 m above the sea level. The vessel sailed from Qingdao of Shandong province (24.5° N, 118.1° E) on 17 March, reached the southernmost area of the cruise near Wenzhou of Zhejiang province on 27 March, and returned at Qingdao (24.5° N, 118.1° E) on 9 April. The study area of the whole cruise covered both the East China Sea and Yellow Sea of China (see Fig. 1).

## 2.2 Instrumentation

The Scanning Mobility Particle Sizer (SMPS, TSI Inc.) system was used to obtain PNDs in the 15–600 nm (mobility diameter) size range at all the 13 sites. The SMPS system includes one Differential Mobility Analyser (DMA) and one Condensation Particle Counter (CPC). The time resolution of this system was 5 min and the flow rates of sample and sheath air were 0.3 and 3.0 L min<sup>-1</sup>, respectively. The relative humidity of sample air was kept below 40% by a silica diffusion dryer within the inlet lines and sheath air cycles. Size-dependent particle losses inside the instruments as well as in the sampling tubes are calculated (Willeke, 1993), and the data are corrected by the obtained correction parameters for each site.

## 2.3 Parameterization

PNDs at each site are parameterized by a multiple log-normal distribution function. Each mode is described by the following function (Seinfeld and Pandis, 1998):

$$\frac{dN_i}{d\log D_p} = \frac{N_i}{\sqrt{2\pi} \log \sigma_i} \exp \left[ -\frac{(\log D_p - \log \mu_i)^2}{2(\log \sigma_i)^2} \right] \quad (1)$$

15158

Title Page

Abstract

Introduction

Conclusions

References

Tables

Figures



Back

Close

Full Screen / Esc

Printer-friendly Version

Interactive Discussion



Where  $N_i$ ,  $\mu_i$  and  $\sigma_i$  are the total number concentration, mean diameter and geometric mean standard deviation of the distribution of mode  $i$ , respectively. The task of the fitting program is to minimize the residual part  $Q$ , which is described as:

$$Q = \int_{15}^{600} \frac{|dN/d\log D_p - \sum_i dN_i/d\log D_p|}{dN/d\log D_p} d\log D_p \quad (2)$$

The growth rate (GR) of newly formed particles and condensational sink (CS) are calculated for NPF events. The CS determines the rapid condensation of gaseous molecules onto the pre-existing aerosols and can be calculated by using Eq. (3).

$$CS = 2\pi D \int_{15}^{600} D_p \beta_M(D_p) n(D_p) d\log D_p = 2\pi D \sum_i \beta_M D_{p,i} N_i \quad (3)$$

Here  $D$  is the diffusion coefficient;  $n(D_p)$  represents the dry particle size distribution function;  $\beta_M$  is the transitional correction factor for the mass flux; and  $N_i$  is the particle number concentration in the size section  $i$ . The CS value in NPF days is calculated as the mean value between 09:00 to 12:00 LT of the day

However, it should be noted that the CS values calculated here are based on the dry particle number size distributions, which may underestimate the real CS values in ambient humidity (Kulmala et al., 2001).

GR is calculated using the Eq. (4):

$$GR = \frac{\Delta D_{p,m}}{\Delta t} \quad (4)$$

Where  $D_{p,m}$  is a mean geometric diameter resulted from the log-normal fitting of the particle number size distribution. The methods for calculating both CS and GR are described by Wu et al. (2007).

|                          |              |
|--------------------------|--------------|
| Title Page               |              |
| Abstract                 | Introduction |
| Conclusions              | References   |
| Tables                   | Figures      |
| ◀                        | ▶            |
| ◀                        | ▶            |
| Back                     | Close        |
| Full Screen / Esc        |              |
| Printer-friendly Version |              |
| Interactive Discussion   |              |



The critical diameter ( $D_{p,crit}$ ) at which 50 % of the particles are activated at the super saturation ( $S_c$ ) can be calculated based on the knowledge of ambient Kappa ( $\kappa$ ) value expressed by Eq. (5) (Petters and Kreidenweis, 2007).

$$\kappa = \frac{4A^3}{27D_{p,crit}^3 \ln^2 S_c} \quad (5)$$

$$A = \frac{4\sigma_{s/a}M_w}{RT\rho_w} \quad (6)$$

Where  $\kappa$  is the hygroscopicity parameter used to model the composition-dependence of the solution water activity;  $\sigma_{s/a}$  is the droplet surface tension (assumed to be that of pure water with a value of  $0.0728 \text{ N m}^{-2}$ );  $M_w$  is the molecular weight of water;  $\rho_w$  is the density of liquid water ( $\text{g cm}^{-3}$ );  $R$  is the universal gas constant ( $\text{J mol}^{-1} \text{ K}^{-1}$ ), and  $T$  is the absolute temperature (K).

### 3 Results and discussion

#### 3.1 Spatial and seasonal variability of PND

The statistics of PNC in the 15–600 nm size range are given in Table 2. Average and median PNCs at all sites were between  $0.5\text{--}2.8 \times 10^4 \text{ cm}^{-3}$  and  $0.4\text{--}2.2 \times 10^4 \text{ cm}^{-3}$ , respectively. The median PNC at urban ( $1.1\text{--}2.2 \times 10^4 \text{ cm}^{-3}$ ) and regional sites ( $0.8\text{--}1.5 \times 10^4 \text{ cm}^{-3}$ ) were two-times larger than those at coastal/background ( $0.4\text{--}0.6 \times 10^4 \text{ cm}^{-3}$ ) and cruise measurement ( $0.5 \times 10^4 \text{ cm}^{-3}$ ). The highest PNCs were observed at UR<sub>u</sub> site due to frequent NPF events, as well as intensive primary emissions, such as coal combustions for local industries, heating supply and residents' use (Li et al., 2008). The average observed PNCs at Chinese urban sites ( $1.8 \times 10^4 \text{ cm}^{-3}$ ) were higher than those in European cities which were reported as  $1.6\text{--}7.0 \times 10^3 \text{ cm}^{-3}$  and  $1.6 \pm 0.8 \times 10^4 \text{ cm}^{-3}$  by Borsos et al. (2012) and Kumar et al. (2013a), respectively, suggesting

**Submicron aerosols  
at thirteen diversified  
sites in China**

J. F. Peng et al.

Title Page

Abstract

Introduction

Conclusions

References

Tables

Figures



Back

Close

Full Screen / Esc

Printer-friendly Version

Interactive Discussion



a much larger exposure risks to Chinese population compared with those in European cities. Meanwhile, the average PNCs in low aerosol-loading area (coastal/background sites) in China were still two-fold higher than those in European countries (A. Asmi et al., 2011). This suggests that the high aerosol loading in the background areas of China increased the background aerosol concentration.

Peak diameters for measured size distributions are calculated in the range of 24–115 nm for urban sites. The largest peak diameters were found at regional sites, which was  $\sim 89$  nm on average. The aging of particles during their transport from urban to regional area was expected, which likely led to the growth of particle diameters (Moffet and Prather, 2009). That, in turn, led to the largest particle peak diameters at regional sites despite the frequent NPF events at these sites. Besides, particle emissions from biomass burning in regional areas had diameter larger than 100 nm (Reid et al., 2005), and might influence the diameter of ambient particles at regional sites. At coastal sites, peaks of particle size distributions were not as sharp as those seen at other sites. Meanwhile, PNCs in these sites show a wide variation near the peak diameters, as both clean background episode and polluted episode caused by transportation occurred in these area (Hu et al., 2013). The median particle size distribution at most of the sites can be fitted into three modes. The peak diameters of these modes ranged from 132–327 nm for the first mode (which can be roughly recognized as accumulation mode), 59–116 nm for the second mode (which can be roughly recognized as Aitken mode), and 17–38 nm for the third mode (which can be roughly recognized as nucleation mode or the second Aitken mode). At  $HS_r$ ,  $CD_r$  and  $ES_s$  sites, the fitting exercise give only the first and second modes.

Strong seasonal variations were found at the  $JX_u$  and  $WX_u$  sites, where the measurements were conducted both in summer and winter. Compared to wintertime, higher PNCs in nucleation mode and lower accumulation modes particles were observed. This is because of the stronger primary emissions during winter time due to local combustion for domestic heating (Wu et al., 2008).

### 3.2 Particle number concentration in different size ranges

The PNCs in the 15–600 nm range are separated into three different size groups, which are smaller than 25 nm ( $N_{15-25}$ ), 25–100 nm ( $N_{25-100}$ ) and 100–600 nm ( $N_{100-600}$ ). These three size groups are used to represent three modes of nucleation, Aitken, and accumulation, respectively. The number concentration in each mode can be approximated by integrating certain size distribution using the Eq. (7):

$$N_{a-b}(t) = \int_a^b n(D_p, t) d \log D_p = \sum_{i=a}^b n_i(D_p, t) \quad (7)$$

Where  $N_{a-b}(t)$  represents PNCs in the  $a$ – $b$  nm range at a certain time interval,  $D_p$  is the geometric mean diameter of the size interval, and  $n_i$  is the measured PNC in a particular size interval ( $\text{cm}^{-3}$ ).

As illustrated in Fig. 3, there were major differences among the distribution of PNCs in different size ranges at individual sites. The PNCs in each size range show a good log-normal distribution in most cases. In our study,  $N_{100-600}$  did not show obvious differences between urban and regional sites, though these values at both types of sites were much larger than those at coastal sites and cruise measurement, indicating the regional feature of secondary aerosols in the whole region of city clusters. Mean  $N_{25-100}$  values appeared to be up to 10-times higher than those in 100–600 nm size range at urban sites, but no significant difference was found at other sites (Fig. 3), indicating the emission from road vehicles at urban sites. Both the distributions of  $N_{15-25}$  and  $N_{25-100}$  show a very “narrow” distribution at most studying sites compared with European countries (A. Asmi et al., 2011), mainly because there were seldom some episodes with very few particles in the atmosphere in China. Even if the air mass was coming from the clean remote continental or oceanic region, the new particle formation and high flux of primary particle emission would increase the  $N_{15-25}$  and  $N_{25-100}$ , respectively, within a short time (Wu et al., 2008). The PNC of nucleation mode ( $N_{15-25}$ ) particles at

coastal sites was lower than those of  $N_{100-600}$  and  $N_{25-100}$ , especially in autumn and winter, suggesting that either the nucleation rate was low, or high proportion of nucleation mode particles coagulated onto the surfaces of larger particles. Besides, a “wide” distribution (Fig. 3c) of  $N_{15-25}$  indicates that though the nucleation rate was low in these sites most of time, a few NPF events with high concentration in nucleation mode still occurred.

### 3.3 Diurnal variation of PND

Figure 4 shows the diurnal variations of the average PND at all the measurement sites. These figures are sorted by seasons and site types. Diurnal PND at nearly all the measurement sites presented a build-up of high concentration belts with peak diameter between 70 and 150 nm. These belts were much more obvious during night time, when there was neither NPF nor large amount of primary emissions, and should be recognized as the accumulation mode. As smaller particles in nucleation mode and Aitken mode have large diffusion coefficient which provide them a large possibility to coagulate onto the surfaces of larger-sized particles, the residence time for particles in the boundary layer are short (Davidson and Wu, 1990). On the other hand, accumulation mode particles had much longer atmospheric life and experienced longer aging process in the atmosphere, resulting in the appearance of this accumulation belt. The higher concentration and larger diameter of particles in this accumulation belts may reflect higher degree of aging of ambient particles. For example, at some sites such as  $YF_r$  and  $KP_r$ , the peaks of these layers were about 100–120 nm, larger than those at the urban sites of  $SH_u$  and  $WX_u$  (about 80–90 nm). Besides, particles at all other sites in the three large city groups (see the black circle in Fig. 1) had these high concentration belts, suggesting that the regional pollution feature within the whole city group area. In contrast, no such accumulation belt was found at  $UR_u$  site, as the PND at  $UR_u$  site was largely influenced by the large primary emissions and NPF.

NPF events at all sites occurred in the middle of the day when solar radiation was strong (Fig. 4). There were large concentrations of nucleation mode particles in the

## Submicron aerosols at thirteen diversified sites in China

J. F. Peng et al.

Title Page

Abstract

Introduction

Conclusions

References

Tables

Figures



Back

Close

Full Screen / Esc

Printer-friendly Version

Interactive Discussion



## Submicron aerosols at thirteen diversified sites in China

J. F. Peng et al.

Title Page

Abstract

Introduction

Conclusions

References

Tables

Figures



Back

Close

Full Screen / Esc

Printer-friendly Version

Interactive Discussion



middle of the day, showing the contribution of the NPF events to the PNC during the whole measurements. As there were much more NPF events in summer time, the contribution to the PNCs were much more obvious. On the other hand, the PNCs of nucleation mode were pretty low at any time of day during both the winter measurement campaigns and some of the autumn measurements since there was no NPF event found (Table 3). Compared with urban and regional sites, influence of PNC at coastal/background sites by NPF events was much lower, due to the lower concentration of precursor gases (e.g.  $\text{SO}_2$ ) at these sites.

Besides the peak of NPF events around the noon, there were another two concentration peaks during morning (between 07:00 and 09:00 LT) and evening (between 17:00 and 20:00 LT) rush hours at most of the urban sites. The appearance of these peaks was due to the primary emissions from vehicles as well as the diurnal change of the height of boundary layers (Lin et al., 2009). The size of these peaks was about 30–70 nm at urban sites (e.g.  $\text{SH}_u$  and  $\text{WX}_u$ ). In the meanwhile, at regional sites there were also these two concentration peaks at the same time of day. The difference is that at regional sites the size of these peaks were much larger (about 70–150 nm) than at urban sites. This reveals the fact that biomass burning in the regional farmland contribute large amount of primary particles (Huang et al., 2011; Reid et al., 2005). Such morning and evening peaks were not found at background sites, confirming that there were no primary emissions near these background sites.

### 3.4 Frequencies and parameters of NPF events

Obvious NPF events were recognized during most of our measurements. The criterion for discerning NPF events in this study includes three steps. First, there should be a burst of PNC in nucleation mode particles below 25 nm in diameter (Birmili and Wiedensohler, 2000). Second, meanwhile, primary emitted species, such as BC and CO concentrations should not enhance significantly. Third, the event should last at least for more than 2 h, with the increase in particle diameter. Two typical types of NPF events (the “banana” and the “apple”, which were classified by Wu et al., 2007) were



observed at a number of our sites. The frequencies of NPF events at urban and regional sites (38 %) were similar to previous studies that focused on the NPF events in some other sites in China (Wu et al., 2007; Yue et al., 2013) and were much higher than at coastal sites and cruise measurement (14 %) during our measurements (Fig. 5).

5 Sulfuric acid is a well-known precursor for nucleation (Boy et al., 2005; Zhang, 2010; Yue et al., 2010; Andreae, 2013). High concentration of SO<sub>2</sub> and OH provides strong source of sulfuric acid at urban and regional sites, and promote the NPF events. On the other hand, the aerosol loading in the ambient atmosphere acts as the condensation and coagulation sink and thus restrain the NPF event. Though high concentration of pre-existing particles could hinder the NPF at urban and regional sites, there were also high precursor concentration (such as SO<sub>2</sub>, and VOCs) and strong oxidation (performed as high O<sub>3</sub> and OH radical concentration) at these sites, which will favor the NPF. At urban and regional sites in our study, the high precursor concentration and strong oxidation may play a more crucial role than the high concentration of pre-existing particles. On the other hand, in the clean coastal area in China, concentrations of procurers as well as the particles are not as high as in urban area as both gases and particles will be dilute during the transport from polluted region to clean coastal area. However, unlike the particles, the gaseous precursors may also undergo continually atmospheric oxidation and transform into particle phase during the transport, which makes the reduction of gaseous precursors larger than the reduction of particles, resulting in fewer NPF events at coastal sites. Besides, other reasons such as meteorological conditions may also affect the frequency of NPF events at diversified sites. In polluted areas, the NPF events are often expected to occur since the air mass is coming from the clean continental background and is not greatly influenced by the polluted urban air (Wu et al., 2007). At coastal sites, no NPF events are expected to take place when the air mass is coming from the ocean side with clean air.

25 In general, CS in NPF days varied from 0.009–0.056 s<sup>-1</sup> at urban sites, 0.003–0.086 s<sup>-1</sup> at regional sites, 0.011–0.026 s<sup>-1</sup> at coastal/background sites and 0.009–0.011 s<sup>-1</sup> during cruise measurement (see Table 3). Upper limit of CS at the polluted

## Submicron aerosols at thirteen diversified sites in China

J. F. Peng et al.

Title Page

Abstract

Introduction

Conclusions

References

Tables

Figures



Back

Close

Full Screen / Esc

Printer-friendly Version

Interactive Discussion



urban and regional area were larger than that in the clean coastal/background and cruise measurement sites, while the lower limit of CS at different sites showed no obvious difference, because there were still some “clean case” NPF events in polluted urban area (Wu et al., 2007).

5 The average GRs of newly formed particles (calculated from 15 nm to 30 nm) were 8.0–10.9 nm h<sup>-1</sup> at urban sites, 7.4–13.6 nm h<sup>-1</sup> at regional sites, and 2.8–7.5 nm h<sup>-1</sup> at both the coastal sites and cruise measurement (see Table 3). The highest GR were found at YF<sub>r</sub> site (regional) with value of 21 nm h<sup>-1</sup>. Average GRs at urban and regional sites were one time higher than GRs at coastal sites and cruise measurement, indicating that the higher gaseous precursors in the polluted area not only favored the formation of particles, but also accelerated the growth rate as long as the nucleation particles are formed.

10 Both the CS and GR results in our study are comparable to other studies performed in Beijing (Wu et al., 2007), Back-garden (Yue et al., 2013), and Xinken (Liu et al., 2008), in China. CS values in our study are generally higher than those at European and American sites and smaller than those at some sites in developing countries, such as New Delhi (see Table 3). The GR values show no obvious differences between China and other countries (both in developed and developing countries) at the same site types (see Table 3).

### 20 3.5 Evaluation of the contribution of NPF to potential CCN

25 The basic idea to estimate the production of potential CCN from NPF events is based on the assumption that particles larger than a certain diameter could be served as CCN. As the newly formed particles consist mainly ammonium sulfate and secondary organics (Yue et al., 2010) and primary emission particles contain a lot of black carbon and hydrophobic organics (Medalia and Rivin, 1982; Reid et al., 2005), the  $\kappa$  value for newly formed particles and primary emission particles may be of large difference. Some previous studies in China have concluded that the average  $\kappa$  value of all ambient particles is about 0.3 for many environments in China (Gunthe et al., 2011; Yue

## Submicron aerosols at thirteen diversified sites in China

J. F. Peng et al.

Title Page

Abstract

Introduction

Conclusions

References

Tables

Figures



Back

Close

Full Screen / Esc

Printer-friendly Version

Interactive Discussion



et al., 2010; Rose et al., 2010), but few has provided the  $\kappa$  value of newly formed particles in the atmosphere. In this study, the hygroscopicity parameter  $\kappa$  for the newly formed particles is taken as 0.43 at about 100 nm based on the assumption of one third of chemical components of these particles are organics and others were inorganics (Gunthe et al., 2011; Yue et al., 2010). Therefore, the only task left is to achieve the PND of newly formed particles.

Mode fitting method was used to distinguish the newly formed particles from others. A total of three (or four) lognormal modes are achieved in the fitness exercise (see Eq. 1) on the PND data averaged over every half an hour. These include up to two NPF modes (with initial diameter about 15–20 nm, which may grow up to 50 nm later), one Aitken mode (40–100 nm) as well as one accumulation mode (100–500 nm). Figure 6 illustrates an example of the mode fitting results at the site of KP<sub>r</sub>, which is a typical regional site with high frequency of NPF events. Diurnal half-hourly average PND data are used for the log-normal fitting. Hourly fitting results in the afternoon from 11:00–16:00 LT at KP<sub>r</sub> site with two NPF modes and two pre-existing modes are shown in Fig. 6. At the site of KP<sub>r</sub>, NPF events occurred between mainly between 09:00 and 11:00 LT every day, resulting in a sharp and narrow nucleation mode peak at about 19 nm at 11:00 LT (Fig. 6). In the following five hours, the peak diameter of NPF mode gradually grew from 19 to 50 nm, with the concentration of NPF mode decreasing from 7500 to 5000 cm<sup>-3</sup> at the same time. As the newly formed particles had log-normal distribution, when peak diameters of the NPF modes are 50 nm, there were some particles that exceeded 80 or even 100 nm diameter. These particles were large enough to possibly act as CCN under a certain S<sub>c</sub>. Therefore, the contribution of NPF to potential CCN concentration can be calculated by integrating the NPF mode with particles diameter larger than D<sub>p,crit</sub>. The advantage of this method is that it can distinguish newly formed particles from the pre-existing particles in the ambient air. However, the method asks for very prominent NPF peak in the size distribution to achieve accurate fitness results. It is challenging to extract NPF mode when the NPF peaks are submerged in the size distribution of ambient particles. Therefore, this method can only be used during

## Submicron aerosols at thirteen diversified sites in China

J. F. Peng et al.

[Title Page](#)[Abstract](#)[Introduction](#)[Conclusions](#)[References](#)[Tables](#)[Figures](#)[Back](#)[Close](#)[Full Screen / Esc](#)[Printer-friendly Version](#)[Interactive Discussion](#)

afternoon from 13:00 to 17:00 LT when the time is neither too early for the formation of new particles, nor too late for primary emission to perform a dominate role in the ambient PND. Therefore our subsequent discussions focus on this time period.

The contributions of NPF and growth to potential CCN concentration in all measurements are calculated using the same method. Results of this exercise are illustrated in Table 4. Two values of super saturations are assumed here as 0.5 and 0.2 %, with critical diameter between 50 and 91 nm for newly formed particles, and between 60 and 100 nm for other particles, respectively. Contributions of NPF to potential CCN concentration varied greatly during different measurements, ranging from 0–66 % when  $S_c$  is 0.5, and 0–24 % when  $S_c$  is 0.2 (Table 4). The highest values were found during the summer at  $WX_u$ . During summer, the average contributions value at urban and regional sites were 50 % ( $S_c = 0.5$ ) and 18 % ( $S_c = 0.2$ ), which were much higher than in other seasons. The strong oxidation condition in summer might favor the formation of new NPF as well as the growth of newly formed particles, accelerating the newly formed particles to perform as CCN. On the contrary, the contribution was zero during two winter measurements, as no NPF events were observed during these measurements.

Weighted average contributions for different size types are roughly calculated. Annual average contribution of NPF to CCN at urban, regional and coastal sites were found to be 33 %, 19 %, 7 % (at  $S_c = 0.5$ ), and 11 %, 6 %, 0 % (at  $S_c = 0.2$ ), respectively. Good correlation ( $R^2 = 0.7$ ) between growth rate of NPF and contribution to CCN among all sties was found, indicating that growth rates of NPF events are the decisive factor in the conversion of newly formed particle to possible CCN (Yue et al., 2011).

Although there were two NPF events during the cruise measurement, no contribution to CCN concentration was found by any of these NPF events, because the diameter of these secondary particles did not meet the critical diameter for CCN. Zhang et al. (2012) have demonstrated in their work that NPF in marine environments is not likely to produce particles of the size of CCN. Our study further confirms that the NPF events showed little impact on the concentration of CCN in the marine area near polluted

Submicron aerosols  
at thirteen diversified  
sites in China

J. F. Peng et al.

Title Page

Abstract

Introduction

Conclusions

References

Tables

Figures



Back

Close

Full Screen / Esc

Printer-friendly Version

Interactive Discussion



continent. It may need more than one day for the newly formed particles to perform as CCN.

In previous studies, the enhancement of CCN concentration obtained by dividing the number of CCN-sized particles after a NPF event by that prior to the event was used to describe the contribution of NPF events to corresponding CCN. The average CCN enhancement factors after the NPF events at  $S_c = 0.2$  ( $D_{p,crit} = 100$  nm) were calculated to be 1.5 at a remote site in Northern Finland (Lihavainen et al., 2003) and in the range of 1.5–2.5 in Beijing (Yue et al., 2011). Similar conclusion was obtained in Botsalano, but with great seasonal variation (Laakso et al., 2013). The factors in these studies are higher than in our study because they only considered NPF days. The values would be much lower and similar to our result if the enhancements were multiplied by the frequencies of NPF events. Besides, the method used in these studies did not consider the influence of primary emissions and change of boundary layer height on CCN concentration (Laakso et al., 2013) and thus may over-estimate the enhancements.

Because all the sites in our study were away from main road and stationary sources, PNC of primary emission were not expected to change much during the focused time intervals. Besides, our mode fit method has considered the non-NPF particles and therefore, our results are not influenced greatly by the primary emissions. However, our approach to calculate the contribution of NPF to CCN also has some uncertainties and limitations. First, we can calculate how much a single NPF events contributed to the CCN. Some of the pre-existing particles before NPF events may also come from the NPF in previous days, but these can only be recognized as pre-existing particles rather than NPF particles in our study. This is likely to result in underestimation of the contribution. Second, some non-NPF particles may have a chance to be recognized as NPF particle when we perform the processing of diurnal average PNCs, which may lead to overestimation of results. Besides, as discussed above, the approach requires very clear NPF peaks in the size distributions in order to achieve accurate fitness results. As a result, the studying time period is constrained between 14:00 and 17:00 LT, when

Submicron aerosols  
at thirteen diversified  
sites in China

J. F. Peng et al.

Title Page

Abstract

Introduction

Conclusions

References

Tables

Figures



Back

Close

Full Screen / Esc

Printer-friendly Version

Interactive Discussion



the NPF mode is clear and evening rush hour has not come. This may lead to an underestimation contribution as it takes time for the newly formed particles to growth into CCN-size. Based on field measurements, our work nevertheless provides annual and seasonal average contribution of NPF events to CCN production for the first time in diversified Chinese atmosphere.

#### 4 Summary and conclusions

This paper presents size-resolved measurements of aerosol particles in the 15–600 nm size range during the 15 individual field campaigns, taken between 2008 and 2011, at thirteen different sites in China. These sites included 5 urban sites, 4 regional sites, 3 coastal/background sites and one ship cruise measurement, and are mainly located within the three largest city clusters of China.

The particle number size distributions were fitted into three modes (nucleation, Aitken, accumulation) at most of the sites. The median PNC at urban ( $1.1\text{--}2.2 \times 10^4 \text{ cm}^{-3}$ ) and regional sites ( $0.8\text{--}1.5 \times 10^4 \text{ cm}^{-3}$ ) are two-times larger than those at coastal and background ( $0.4\text{--}0.6 \times 10^4 \text{ cm}^{-3}$ ) sites and cruise measurement ( $0.5 \times 10^4 \text{ cm}^{-3}$ ).

Primary emission from road vehicles as well as regional biomass burning appears to have a large contribution to the ambient PNCs. High emissions from road vehicles at urban sites resulted in up to 10-times higher  $N_{25\text{--}100}$  than those of  $N_{100\text{--}600}$ . PNCs in both these size ranges were nearly identical at all other sites. Vehicular emissions at urban sites and biomass burning emission at regional sites led to two concentration peaks in the early morning and evening hours.

Regional secondary aerosol pollution is a main feature for the submicron aerosol pollution in China. No obvious differences in the  $N_{100\text{--}600}$  particles were observed between urban and regional sites. Diurnal variations show a build-up of high concentration accumulation belt at all the regional sites.

### Submicron aerosols at thirteen diversified sites in China

J. F. Peng et al.

Title Page

Abstract

Introduction

Conclusions

References

Tables

Figures



Back

Close

Full Screen / Esc

Printer-friendly Version

Interactive Discussion



**Submicron aerosols  
at thirteen diversified  
sites in China**

J. F. Peng et al.

Title Page

Abstract

Introduction

Conclusions

References

Tables

Figures



Back

Close

Full Screen / Esc

Printer-friendly Version

Interactive Discussion



The occurrence frequencies of the NPF events in high aerosol-loading environment of China were found to be higher than those in less aerosol-loading environments. High gaseous precursors and strong oxidation at urban and regional sites not only found to favor the formation of particles, but also accelerate the growth rate after the nucleation mode particles are formed. The average GR of nucleation mode particles were 8.0–10.9 nm h<sup>-1</sup> at urban sites, 7.4–13.6 nm h<sup>-1</sup> at regional sites and 2.8–7.5 nm h<sup>-1</sup> at coastal sites and cruise measurement. The NPF events in the less aerosol-loading environment were found to be greatly influenced by pollutant transport.

Average contributions of NPF events to potential CCN are calculated in this study. Contributions of NPF events to potential CCN at 0.2 super-saturation in the afternoon of all measurement days were 11 % and 6 % at urban sites and regional sites, respectively. On the other hand, NPF events at coastal sites and cruise measurement had little impact on potential CCN.

Our study presents a unique dataset of aerosol size distributions and general concepts of the features of submicron particle pollution along with the fundamental drivers of particulate pollution in China. Besides, our estimation of contribution of NPF events to corresponding CCN might be particularly useful for the validation of global climate models.

**The Supplement related to this article is available online at  
doi:10.5194/acpd-14-15149-2014-supplement.**

*Acknowledgements.* This work was supported by the National Natural Science Foundation of China (21025728 and 21190052), the National Basic Research Program of China (2013CB228503) and the China Ministry of Environmental Protection's Special Funds for Scientific Research on Public Welfare (201009002). Prashant Kumar, Jianfei Peng and Min Hu thank the University of Surrey's International Relations Office for the Santander Postgraduate Mobility Award that helped Jianfei Peng to visit University of Surrey, UK, to develop this research article collaboratively.



## References

- Andreae, M. O.: The aerosol nucleation puzzle, *Science*, 339, 911–912, doi:10.1126/science.1233798, 2013.
- Asmi, A., Wiedensohler, A., Laj, P., Fjaeraa, A.-M., Sellegri, K., Birmili, W., Weingartner, E., Baltensperger, U., Zdimal, V., Zikova, N., Putaud, J.-P., Marinoni, A., Tunved, P., Hansson, H.-C., Fiebig, M., Kivekäs, N., Lihavainen, H., Asmi, E., Ulevicius, V., Aalto, P. P., Swietlicki, E., Kristensson, A., Mihalopoulos, N., Kalivitis, N., Kalapov, I., Kiss, G., de Leeuw, G., Henzing, B., Harrison, R. M., Beddows, D., O'Dowd, C., Jennings, S. G., Flentje, H., Weinhold, K., Meinhardt, F., Ries, L., and Kulmala, M.: Number size distributions and seasonality of submicron particles in Europe 2008–2009, *Atmos. Chem. Phys.*, 11, 5505–5538, doi:10.5194/acp-11-5505-2011, 2011.
- Asmi, E., Kivekäs, N., Kerminen, V.-M., Komppula, M., Hyvärinen, A.-P., Hatakka, J., Viisanen, Y., and Lihavainen, H.: Secondary new particle formation in Northern Finland Pallas site between the years 2000 and 2010, *Atmos. Chem. Phys.*, 11, 12959–12972, doi:10.5194/acp-11-12959-2011, 2011.
- Bigi, A. and Ghermandi, G.: Particle number size distribution and weight concentration of background urban aerosol in a Po Valley site, *Water Air Soil Poll.*, 220, 265–278, doi:10.1007/s11270-011-0752-6, 2011.
- Borsos, T., Rimnacova, D., Zdimal, V., Smolik, J., Wagner, Z., Weidinger, T., Burkart, J., Steiner, G., Reischl, G., Hitzengerger, R., Schwarz, J., and Salma, I.: Comparison of particulate number concentrations in three Central European capital cities, *Sci. Total Environ.*, 433, 418–426, 2012.
- Boy, M., Kulmala, M., Ruuskanen, T. M., Pihlatie, M., Reissell, A., Aalto, P. P., Keronen, P., Dal Maso, M., Hellen, H., Hakola, H., Jansson, R., Hanke, M., and Arnold, F.: Sulphuric acid closure and contribution to nucleation mode particle growth, *Atmos. Chem. Phys.*, 5, 863–878, doi:10.5194/acp-5-863-2005, 2005.
- Buseck, P. R. and Adachi, K.: Nanoparticles in the atmosphere, *Elements*, 4, 389–394, doi:10.2113/gselements.4.6.389, 2008.
- Creamean, J. M., Ault, A. P., Ten Hoeve, J. E., Jacobson, M. Z., Roberts, G. C., and Prather, K. A.: Measurements of aerosol chemistry during new particle formation events at a remote rural mountain site, *Environ. Sci. Technol.*, 45, 8208–8216, 2011.

ACPD

14, 15149–15189, 2014

## Submicron aerosols at thirteen diversified sites in China

J. F. Peng et al.

Title Page

Abstract

Introduction

Conclusions

References

Tables

Figures



Back

Close

Full Screen / Esc

Printer-friendly Version

Interactive Discussion





**Submicron aerosols  
at thirteen diversified  
sites in China**

J. F. Peng et al.

Title Page

Abstract

Introduction

Conclusions

References

Tables

Figures



Back

Close

Full Screen / Esc

Printer-friendly Version

Interactive Discussion



Dal Maso, M., Kulmala, M., Riipinen, I., Wagner, R., Hussein, T., Aalto, P. P., and Lehtinen, K. E. J.: Formation and growth of fresh atmospheric aerosols: eight years of aerosol size distribution data from SMEAR II, Hyytiälä, Finland, *Boreal Environ. Res.*, 10, 323–336, 2005.

Davidson, C. I. and Wu, Y. L.: Dry deposition of particles and vapors, in: *Acid Precipitation*, Vol. 3, edited by: Lindberg, S. E., Page, A. L., and Norton, S. A., Springer-Verlag, Berlin, 103–209, 1990.

Du, J. F., Cheng, T. T., Zhang, M., Chen, J. M., He, Q. S., Wang, X. M., Zhang, R. J., Tao, J., Huang, G. H., Li, X., and Zha, S. P.: Aerosol size spectra and particle formation events at urban Shanghai in Eastern China, *Aerosol Air Qual. Res.*, 12, 1362–1372, 2012.

Dunn, M. J., Jimenez, J. L., Baumgardner, D., Castro, T., McMurry, P. H., and Smith, J. N.: Measurements of Mexico City nanoparticle size distributions: observations of new particle formation and growth, *Geophys. Res. Lett.*, 31, L10102, doi:10.1029/2004GL019483, 2004

Dusek, U.: Size matters more than chemistry for cloud-nucleating ability of aerosol particles, *Science*, 312, 1375–1378, doi:10.1126/science.1125261, 2006.

Gao, J., Chai, F. H., Wang, T., and Wang, W. X.: Particle number size distribution and new particle formation (NPF) in Lanzhou, Western China, *Particuology*, 9, 611–618, 2011.

Gong, Z. H., Lan, Z. J., Xue, L., Zeng, L. W., He, L. Y., and Huang, X. F.: Characterization of submicron aerosols in the urban outflow of the central Pearl River Delta region of China, *Frontiers of Environmental Science & Engineering*, 6, 725–733, 2012.

Gunthe, S. S., Rose, D., Su, H., Garland, R. M., Achtert, P., Nowak, A., Wiedensohler, A., Kuwata, M., Takegawa, N., Kondo, Y., Hu, M., Shao, M., Zhu, T., Andreae, M. O., and Pöschl, U.: Cloud condensation nuclei (CCN) from fresh and aged air pollution in the megacity region of Beijing, *Atmos. Chem. Phys.*, 11, 11023–11039, doi:10.5194/acp-11-11023-2011, 2011.

Guo, S., Hu, M., Wang, Z. B., Slanina, J., and Zhao, Y. L.: Size-resolved aerosol water-soluble ionic compositions in the summer of Beijing: implication of regional secondary formation, *Atmos. Chem. Phys.*, 10, 947–959, doi:10.5194/acp-10-947-2010, 2010.

Hamed, A., Joutsensaari, J., Mikkonen, S., Sogacheva, L., Dal Maso, M., Kulmala, M., Cavalli, F., Fuzzi, S., Facchini, M. C., Decesari, S., Mircea, M., Lehtinen, K. E. J., and Laaksonen, A.: Nucleation and growth of new particles in Po Valley, Italy, *Atmos. Chem. Phys.*, 7, 355–376, doi:10.5194/acp-7-355-2007, 2007.

**Submicron aerosols  
at thirteen diversified  
sites in China**

J. F. Peng et al.

Title Page

Abstract

Introduction

Conclusions

References

Tables

Figures



Back

Close

Full Screen / Esc

Printer-friendly Version

Interactive Discussion



- Harrison, R. M., Beddows, D. C. S., and Dall'Osto, M.: PMF analysis of wide-range particle size spectra collected on a major highway, *Environ. Sci. Technol.*, 45, 5522–5528, 2011.
- Heal, M. R., Kumar, P., and Harrison, R. M.: Particles, air quality, policy and health, *Chem. Soc. Rev.*, 41, 6606–6630, 2012.
- 5 Hu, W. W., Hu, M., Yuan, B., Jimenez, J. L., Tang, Q., Peng, J. F., Hu, W., Shao, M., Wang, M., Zeng, L. M., Wu, Y. S., Gong, Z. H., Huang, X. F., and He, L. Y.: Insights on organic aerosol aging and the influence of coal combustion at a regional receptor site of central eastern China, *Atmos. Chem. Phys.*, 13, 10095–10112, doi:10.5194/acp-13-10095-2013, 2013.
- 10 Huang, X.-F., He, L.-Y., Hu, M., Canagaratna, M. R., Kroll, J. H., Ng, N. L., Zhang, Y.-H., Lin, Y., Xue, L., Sun, T.-L., Liu, X.-G., Shao, M., Jayne, J. T., and Worsnop, D. R.: Characterization of submicron aerosols at a rural site in Pearl River Delta of China using an Aerodyne High-Resolution Aerosol Mass Spectrometer, *Atmos. Chem. Phys.*, 11, 1865–1877, doi:10.5194/acp-11-1865-2011, 2011.
- 15 Huang, X.-F., He, L.-Y., Xue, L., Sun, T.-L., Zeng, L.-W., Gong, Z.-H., Hu, M., and Zhu, T.: Highly time-resolved chemical characterization of atmospheric fine particles during 2010 Shanghai World Expo, *Atmos. Chem. Phys.*, 12, 4897–4907, doi:10.5194/acp-12-4897-2012, 2012.
- Iida, K., Stolzenburg, M. R., McMurry, P. H., and Smith, J. N.: Estimating nanoparticle growth rates from size-dependent charged fractions: analysis of new particle formation events in Mexico City, *J. Geophys. Res.-Atmos.*, 113, D05207, doi:10.1029/2007JD009260, 2008.
- 20 IPCC (Intergovernmental Panel on Climate Change): Climate Change 2007: The Physical Science Basis. Contribution of Working Group I to the Fourth Assessment, Report of the Intergovernmental Panel on Climate Change, Cambridge University Press, Cambridge, United Kingdom, and New York, NY, USA.
- Kerminen, V.-M., Paramonov, M., Anttila, T., Riipinen, I., Fountoukis, C., Korhonen, H., Asmi, E., Laakso, L., Lihavainen, H., Swietlicki, E., Svenningsson, B., Asmi, A., Pandis, S. N., Kulmala, M., and Petäjä, T.: Cloud condensation nuclei production associated with atmospheric nucleation: a synthesis based on existing literature and new results, *Atmos. Chem. Phys.*, 12, 12037–12059, doi:10.5194/acp-12-12037-2012, 2012.
- 25 Kuang, C., McMurry, P. H., and McCormick, A. V.: Determination of cloud condensation nuclei production from measured new particle formation events, *Geophys. Res. Lett.*, 36, L09822, doi:10.1029/2009GL037584, 2009.
- 30

## Submicron aerosols at thirteen diversified sites in China

J. F. Peng et al.

Title Page

Abstract

Introduction

Conclusions

References

Tables

Figures



Back

Close

Full Screen / Esc

Printer-friendly Version

Interactive Discussion



- Kulmala, M., Dal Maso, M., Makela, J. M., Pirjola, L., Vakeva, M., Aalto, P., Miiikkulainen, P., Hameri, K., O'Dowd, C. D.: On the formation, growth and composition of nucleation mode particles, *Tellus B*, 53, 479–490, 2001.
- 5 Kulmala, M., Kontkanen, J., Junninen, H., Lehtipalo, K., Manninen, H. E., Nieminen, T., Petaja, T., Sipila, M., Schobesberger, S., Rantala, P., Franchin, A., Jokinen, T., Jarvinen, E., Aijala, M., Kangasluoma, J., Hakala, J., Aalto, P. P., Paasonen, P., Mikkila, J., Vanhanen, J., Aalto, J., Hakola, H., Makkonen, U., Ruuskanen, T., Mauldin, R. L., Duplissy, J., Vehkamaki, H., Back, J., Kortelainen, A., Riipinen, I., Kurten, T., Johnston, M. V., Smith, J. N., Ehn, M., Mentel, T. F., Lehtinen, K. E. J., Laaksonen, A., Kerminen, V. M., and Worsnop, D. R.: Direct observations of atmospheric aerosol nucleation, *Science*, 339, 943–946, doi:10.1126/science.1227385, 2013.
- 10 Kumar, P., Robins, A., Vardoulakis, S., and Britter, R.: A review of the characteristics of nanoparticles in the urban atmosphere and the prospects for developing regulatory controls, *Atmos. Environ.*, 44, 5035–5052, 2010.
- 15 Kumar, P., Gurjar, B. R., Nagpure, A., and Harrison, R. H.: Preliminary estimates of particle number emissions from road vehicles in megacity Delhi and associated health impacts, *Environ. Sci. Technol.*, 45, 5514–5521, 2011.
- Kumar, P., Morawska, L., and Harrison, R. M.: Nanoparticles in European cities and associated health impacts, in: *Urban Air Quality in Europe: The Handbook of Environmental Chemistry*, edited by: Viana, M., Vol. 26, Springer, Berlin, Heidelberg, 339–365, doi:10.1007/698\_2012\_161, 2013a.
- 20 Kumar, P., Pirjola, L., Ketzel, M., and Harrison, R. M.: Nanoparticle emissions from 11 non-vehicle exhaust sources – a review, *Atmos. Environ.*, 67, 252–277, 2013b.
- Kumar, P., Morawska, L., Birmili, W., Paasonen, P., Hu, M., Kulmala, M., Harrison, R. M., Norford, L., and Britter, R.: Ultrafine particles in cities, *Environ. Int.*, 66, 1–10, 2014.
- 25 Laakso, L., Merikanto, J., Vakkari, V., Laakso, H., Kulmala, M., Molefe, M., Kgabi, N., Mabaso, D., Carslaw, K. S., Spracklen, D. V., Lee, L. A., Reddington, C. L., and Kerminen, V. M.: Boundary layer nucleation as a source of new CCN in savannah environment, *Atmos. Chem. Phys.*, 13, 1957–1972, doi:10.5194/acp-13-1957-2013, 2013.
- 30 Li, J., Zhuang, G. S., Huang, K., Lin, Y. F., Xu, C., and Yu, S. L.: Characteristics and sources of air-borne particulate in Urumqi, China, the upstream area of Asia dust, *Atmos. Environ.*, 42, 776–787, 2008.

**Submicron aerosols  
at thirteen diversified  
sites in China**

J. F. Peng et al.

Title Page

Abstract

Introduction

Conclusions

References

Tables

Figures



Back

Close

Full Screen / Esc

Printer-friendly Version

Interactive Discussion



- Lihavainen, H., Kerminen, V. M., Komppula, M., Hatakka, J., Aaltonen, V., Kulmala, M., and Viisanen, Y.: Production of “potential” cloud condensation nuclei associated with atmospheric new-particle formation in northern Finland, *J. Geophys. Res.-Atmos.*, 108, 4782, doi:10.1029/2003jd003887, 2003.
- 5 Lin, M., Holloway, T., Oki, T., Streets, D. G., and Richter, A.: Multi-scale model analysis of boundary layer ozone over East Asia, *Atmos. Chem. Phys.*, 9, 3277–3301, doi:10.5194/acp-9-3277-2009, 2009.
- Lin, P., Hu, M., Wu, Z., Niu, Y., and Zhu, T.: Marine aerosol size distributions in the springtime over China adjacent seas, *Atmos. Environ.*, 41, 6784–6796, 2007.
- 10 Liu, S., Hu, M., Wu, Z. J., Wehner, B., Wiedensohler, A., and Cheng, Y. F.: Aerosol number size distribution and new particle formation at a rural/coastal site in Pearl River Delta (PRD) of China, *Atmos. Environ.*, 42, 6275–6283, 2008.
- Medalia, A. I. and Rivin, D.: Particulate carbon and other components of soot and carbon-black, *Carbon*, 20, 481–492, doi:10.1016/0008-6223(82)90084-7, 1982.
- 15 Merikanto, J., Spracklen, D. V., Mann, G. W., Pickering, S. J., and Carslaw, K. S.: Impact of nucleation on global CCN, *Atmos. Chem. Phys.*, 9, 8601–8616, doi:10.5194/acp-9-8601-2009, 2009.
- Moffet, R. C. and Prather, K. A.: In-situ measurements of the mixing state and optical properties of soot with implications for radiative forcing estimates, *P. Natl. Acad. Sci. USA*, 106, 11872–11877, 2009.
- 20 Mönkkönen, P., Koponen, I. K., Lehtinen, K. E. J., Hämeri, K., Uma, R., and Kulmala, M.: Measurements in a highly polluted Asian mega city: observations of aerosol number size distribution, modal parameters and nucleation events, *Atmos. Chem. Phys.*, 5, 57–66, doi:10.5194/acp-5-57-2005, 2005.
- 25 Nel, A., Xia, T., Madler, L., and Li, N.: Toxic potential of materials at the nanolevel, *Science*, 311, 622–627, 2006.
- Petters, M. D. and Kreidenweis, S. M.: A single parameter representation of hygroscopic growth and cloud condensation nucleus activity, *Atmos. Chem. Phys.*, 7, 1961–1971, doi:10.5194/acp-7-1961-2007, 2007.
- 30 Reid, J. S., Koppmann, R., Eck, T. F., and Eleuterio, D. P.: A review of biomass burning emissions part II: intensive physical properties of biomass burning particles, *Atmos. Chem. Phys.*, 5, 799–825, doi:10.5194/acp-5-799-2005, 2005.

**Submicron aerosols  
at thirteen diversified  
sites in China**

J. F. Peng et al.

[Title Page](#)[Abstract](#)[Introduction](#)[Conclusions](#)[References](#)[Tables](#)[Figures](#)[Back](#)[Close](#)[Full Screen / Esc](#)[Printer-friendly Version](#)[Interactive Discussion](#)

Salma, I., Borsós, T., Weidinger, T., Aalto, P., Hussein, T., Dal Maso, M., and Kulmala, M.: Production, growth and properties of ultrafine atmospheric aerosol particles in an urban environment, *Atmos. Chem. Phys.*, 11, 1339–1353, doi:10.5194/acp-11-1339-2011, 2011.

See, S. W., Balasubramanian, R., and Wang, W.: A study of the physical, chemical, and optical properties of ambient aerosol particles in Southeast Asia during hazy and nonhazy days, *J. Geophys. Res.-Atmos.*, 111, D10S08, doi:10.1029/2005jd006180, 2006.

Seinfeld, J. H. and Pandis, S. N.: *Atmospheric Chemistry and Physics. From Air Pollution to Climate Change*, John Wiley & Sons, New York, 429–443, 1998.

Shen, X. J., Sun, J. Y., Zhang, Y. M., Wehner, B., Nowak, A., Tuch, T., Zhang, X. C., Wang, T. T., Zhou, H. G., Zhang, X. L., Dong, F., Birmili, W., and Wiedensohler, A.: First long-term study of particle number size distributions and new particle formation events of regional aerosol in the North China Plain, *Atmos. Chem. Phys.*, 11, 1565–1580, doi:10.5194/acp-11-1565-2011, 2011.

Reid, J. S., Eck, T. F., Christopher, S. A., Koppmann, R., Dubovik, O., Eleuterio, D. P., Holben, B. N., Reid, E. A., and Zhang, J.: A review of biomass burning emissions part III: intensive optical properties of biomass burning particles, *Atmos. Chem. Phys.*, 5, 827–849, doi:10.5194/acp-5-827-2005, 2005.

Rose, D., Nowak, A., Achtert, P., Wiedensohler, A., Hu, M., Shao, M., Zhang, Y., Andreae, M. O., and Pöschl, U.: Cloud condensation nuclei in polluted air and biomass burning smoke near the mega-city Guangzhou, China – Part 1: Size-resolved measurements and implications for the modeling of aerosol particle hygroscopicity and CCN activity, *Atmos. Chem. Phys.*, 10, 3365–3383, doi:10.5194/acp-10-3365-2010, 2010.

Wang, Z. B., Hu, M., Sun, J. Y., Wu, Z. J., Yue, D. L., Shen, X. J., Zhang, Y. M., Pei, X. Y., Cheng, Y. F., and Wiedensohler, A.: Characteristics of regional new particle formation in urban and regional background environments in the North China Plain, *Atmos. Chem. Phys.*, 13, 12495–12506, doi:10.5194/acp-13-12495-2013, 2013a.

Wang, Z. B., Hu, M., Yue, D. L., He, L. Y., Huang, X. F., Yang, Q., Zheng, J., Zhang, R. Y., and Zhang, Y. H.: New particle formation in the presence of a strong biomass burning episode at a downwind rural site in PRD, China, *Tellus B*, 65, 19965, doi:10.3402/tellusb.v65i0.19965, 2013b.

Wehner, B. and Wiedensohler, A.: Long term measurements of submicrometer urban aerosols: statistical analysis for correlations with meteorological conditions and trace gases, *Atmos. Chem. Phys.*, 3, 867–879, doi:10.5194/acp-3-867-2003, 2003.

## Submicron aerosols at thirteen diversified sites in China

J. F. Peng et al.

Title Page

Abstract

Introduction

Conclusions

References

Tables

Figures



Back

Close

Full Screen / Esc

Printer-friendly Version

Interactive Discussion



Wehner, B., Wiedensohler, A., Tuch, T. M., Wu, Z. J., Hu, M., Slanina, J., and Kiang, C. S.: Variability of the aerosol number size distribution in Beijing, China: new particle formation, dust storms, and high continental background, *Geophys. Res. Lett.*, 31, L22108, doi:10.1029/2004GL021596, 2004.

5 WHO: Review of evidence on health aspects of air pollution – REVIHAAP. World Health Organisation, Regional Office for Europe, available at: [http://www.euro.who.int/\\_\\_data/assets/pdf\\_file/0020/182432/e96762-final.pdf](http://www.euro.who.int/__data/assets/pdf_file/0020/182432/e96762-final.pdf) (last access: 5 June 2014), 2013.

10 Wiedensohler, A., Cheng, Y. F., Nowak, A., Wehner, B., Achtert, P., Berghof, M., Birmili, W., Wu, Z. J., Hu, M., Zhu, T., Takegawa, N., Kita, K., Kondo, Y., Lou, S. R., Hofzumahaus, A., Holland, F., Wahner, A., Gunthe, S. S., Rose, D., Su, H., and Poschl, U.: Rapid aerosol particle growth and increase of cloud condensation nucleus activity by secondary aerosol formation and condensation: a case study for regional air pollution in northeastern China, *J. Geophys. Res.-Atmos.*, 114, D00G08, doi:10.1029/2008JD010884, 2009.

15 Willeke, K. and Baron, P. A.: *Aerosol Measurement Principles, Techniques, and Applications*, Van Nostrand Reinhold, Hoboken, NJ, 1993.

Wu, Z. J., Hu, M., Liu, S., Wehner, B., Bauer, S., Ssling, A. M., Wiedensohler, A., Petaja, T., Dal Maso, M., and Kulmala, M.: New particle formation in Beijing, China: statistical analysis of a 1-year data set, *J. Geophys. Res.-Atmos.*, 112, D09209, doi:10.1029/2006JD007406, 2007.

20 Wu, Z. J., Hu, M., Lin, P., Liu, S., Wehner, B., and Wiedensohler, A.: Particle number size distribution in the urban atmosphere of Beijing, China, *Atmos. Environ.*, 42, 7967–7980, 2008.

Xu, P., Chen, Y. F., and Ye, X. J.: Haze, air pollution, and health in China, *Lancet*, 382, 2067–2067, 2013.

25 Yli-Juuti, T., Riipinen, I., Aalto, P. P., Nieminen, T., Maenhaut, W., Janssens, I. A., Claeys, M., Salma, I., Ocskay, R., Hoffer, A., Imre, K., and Kulmala, M.: Characteristics of new particle formation events and cluster ions at K-puszta, Hungary, *Boreal Environ. Res.*, 14, 683–698, 2009.

Yu, F., Luo, G., Liu, X., Easter, R. C., Ma, X., and Ghan, S. J.: Indirect radiative forcing by ion-mediated nucleation of aerosol, *Atmos. Chem. Phys.*, 12, 11451–11463, doi:10.5194/acp-12-11451-2012, 2012.

30 Yue, D. L., Hu, M., Zhang, R. Y., Wang, Z. B., Zheng, J., Wu, Z. J., Wiedensohler, A., He, L. Y., Huang, X. F., and Zhu, T.: The roles of sulfuric acid in new particle formation and growth in the

mega-city of Beijing, *Atmos. Chem. Phys.*, 10, 4953–4960, doi:10.5194/acp-10-4953-2010, 2010.

Yue, D. L., Hu, M., Zhang, R. Y., Wu, Z. J., Su, H., Wang, Z. B., Peng, J. F., He, L. Y., Huang, X. F., Gong, Y. G., and Wiedensohler, A.: Potential contribution of new particle formation to cloud condensation nuclei in Beijing, *Atmos. Environ.*, 45, 6070–6077, 2011.

Yue, D. L., Hu, M., Wang, Z. B., Wen, M. T., Guo, S., Zhong, L. J., Wiedensohler, A., and Zhang, Y. H.: Comparison of particle number size distributions and new particle formation between the urban and rural sites in the PRD region, China, *Atmos. Environ.*, 76, 181–188, 2013.

Zhang, R. Y.: Getting to the critical nucleus of aerosol formation, *Science*, 328, 1366–1367, 2010.

Zhang, R. Y., Khalizov, A., Wang, L., Hu, M., and Xu, W.: Nucleation and growth of nanoparticles in the atmosphere, *Chem. Rev.*, 112, 1957–2011, 2012.

Zhang, Y. H., Hu, M., Zhong, L. J., Wiedensohler, A., Liu, S. C., Andreae, M. O., Wang, W., and Fan, S. J.: Regional integrated experiments on air quality over Pearl River Delta 2004 (PRIDE-PRD2004): overview, *Atmos. Environ.*, 42, 6157–6173, 2008.

## Submicron aerosols at thirteen diversified sites in China

J. F. Peng et al.

Title Page

Abstract

Introduction

Conclusions

References

Tables

Figures



Back

Close

Full Screen / Esc

Printer-friendly Version

Interactive Discussion



## Submicron aerosols at thirteen diversified sites in China

J. F. Peng et al.

**Table 1.** Summary of information providing description of sampling periods at each measurement site. Please note that the words in parenthesis against each site represent a short name of each site, and subscripts u, r, c and s indicate urban, regional, background/coastal and cruise site types, respectively.

| Type                | Sites                             | Coordinates             | Sampling period    | Valid data    |
|---------------------|-----------------------------------|-------------------------|--------------------|---------------|
| Urban               | Guangzhou (GZ <sub>u</sub> )      | 23.13° N, 113.26° E     | 12–29 Nov 2010     | 4766          |
|                     | Shanghai (SH <sub>u</sub> )       | 31.23° N, 21.53° E      | 15 Apr–22 Jun 2010 | 18 658        |
|                     | Urumchi (UC <sub>u</sub> )        | 87.58° N, 43.83° E      | 16 May–2 Jun 2008  | 4835          |
|                     | Wuxi (WX <sub>u</sub> )           | 31.56° N, 120.29° E     | 21 Jul–7 Aug 2010  | 4769          |
|                     |                                   |                         | 1–14 Jan 2011      | 4926          |
|                     | Jinhua (JH <sub>u</sub> )         | 29.1° N, 119.69° E      | 29 Oct–28 Nov 2011 | 7776          |
| Regional            | Heshan (HS <sub>r</sub> )         | 22.71° N, 112.93° E     | 12–29 Nov 2010     | 4921          |
|                     | Kaiping (KP <sub>r</sub> )        | 22.33° N, 112.54° E     | 18 Oct–17 Nov 2008 | 8465          |
|                     | Jiaxing (JX <sub>r</sub> )        | 30.8° N, 120.8° E       | 28 Jun–15 Jul 2010 | 4564          |
|                     |                                   |                         | 5–22 Dec 2010      | 4030          |
|                     |                                   | Yufa (YF <sub>r</sub> ) | 39.51° N, 116.3° E | 5–31 Oct 2007 |
| Coastal/ Background | Baguang (BG <sub>c</sub> )        | 22.65° N, 114.54° E     | 25 Oct–3 Dec 2009  | 5895          |
|                     | Wenling (WL <sub>c</sub> )        | 28.40° N, 121.61° E     | 30 Oct–28 Nov 2011 | 7064          |
|                     | Changdao (CD <sub>c</sub> )       | 37.99° N, 120.70° E     | 19 Mar–24 Apr 2011 | 10 338        |
| Cruise              | East China Sea (ES <sub>s</sub> ) | –                       | 18 Mar–8 Apr 2011  | 5015          |

Title Page

Abstract

Introduction

Conclusions

References

Tables

Figures



Back

Close

Full Screen / Esc

Printer-friendly Version

Interactive Discussion





Submicron aerosols  
at thirteen diversified  
sites in China

J. F. Peng et al.

**Table 2.** Particle diameter, percentile of total PNCs and modal fit parameters for median size distributions at each site.  $\sigma$  is the geometric standard deviation of the mode,  $N_m$  is the mode number concentration,  $D_{p,m}$  is the geometric mean diameter of the fitted log-normal mode.

| Type                   | Sites               | Peak diameter (nm) | Number Concentration (cm <sup>-3</sup> ) |      |        |        |        | Fitted mode 1 |                |                           | Fitted mode 2 |                |                           | Fitted mode 3 |                |                           |          |
|------------------------|---------------------|--------------------|--|------|--------|--------|--------|---------------|----------------|---------------------------|---------------|----------------|---------------------------|---------------|----------------|---------------------------|----------|
|                        |                     |                    | Average                                  | 5%   | 16%    | 50%    | 84%    | 95%           | $D_{p,m}$ (nm) | $N_m$ (cm <sup>-3</sup> ) | $\sigma$      | $D_{p,m}$ (nm) | $N_m$ (cm <sup>-3</sup> ) | $\sigma$      | $D_{p,m}$ (nm) | $N_m$ (cm <sup>-3</sup> ) | $\sigma$ |
| Urban                  | GZ <sub>u</sub>     | 85                 | 13 716                                   | 5222 | 6939   | 11 563 | 20 192 | 29 838        | 166            | 3078                      | 1.60          | 65             | 5404                      | 1.72          | 17             | 5621                      | 1.82     |
|                        | SH <sub>u</sub>     | 40                 | 12 931                                   | 4195 | 5903   | 10 560 | 19 746 | 28 986        | 218            | 917                       | 1.49          | 71             | 5863                      | 1.7           | 25             | 4449                      | 1.55     |
|                        | UR <sub>u</sub>     | 24                 | 28 421                                   | 6663 | 10 977 | 22 415 | 45 214 | 70 341        | 146            | 555                       | 1.89          | 59             | 7122                      | 1.83          | 24             | 18 910                    | 1.73     |
|                        | WX <sub>u_win</sub> | 52                 | 19 465                                   | 5818 | 8556   | 16 046 | 29 533 | 47 583        | 142            | 4972                      | 1.60          | 63             | 9878                      | 1.67          | 29             | 1250                      | 1.33     |
|                        | WX <sub>u_sum</sub> | 73                 | 17 396                                   | 7710 | 10 572 | 16 051 | 23 794 | 31 408        | 154            | 2092                      | 1.61          | 61             | 7844                      | 1.6           | 23             | 7473                      | 1.59     |
|                        | JH <sub>u</sub>     | 115                | 14 331                                   | 5029 | 6848   | 12 809 | 21 328 | 29 956        | 329            | 206                       | 1.23          | 116            | 10 753                    | 1.71          | 36             | 1892                      | 1.52     |
| Regional               | HS <sub>r</sub>     | 72                 | 16 076                                   | 7548 | 9635   | 15 084 | 22 230 | 27 898        | 134            | 5784                      | 1.61          | 59             | 9252                      | 1.63          | –              | –                         | –        |
|                        | KP <sub>r</sub>     | 93                 | 11 170                                   | 2587 | 4177   | 7900   | 16 520 | 32 707        | 327            | 311                       | 1.40          | 95             | 6883                      | 1.81          | 17             | 1280                      | 1.76     |
|                        | JX <sub>r_sum</sub> | 68                 | 16 593                                   | 5320 | 7799   | 13 033 | 23 059 | 40 126        | 197            | 1482                      | 1.56          | 84             | 5560                      | 1.56          | 25             | 7690                      | 1.86     |
|                        | JX <sub>r_win</sub> | 87                 | 13 610                                   | 3588 | 5700   | 11 737 | 20 917 | 30 128        | 138            | 4946                      | 1.59          | 74             | 2460                      | 1.38          | 38             | 4451                      | 1.56     |
|                        | YF <sub>r</sub>     | 123                | 10 195                                   | 2259 | 4033   | 8761   | 15 610 | 23 455        | 150            | 5715                      | 1.83          | 66             | 1831                      | 1.58          | 26             | 1436                      | 1.66     |
| Coastal/<br>background | BG <sub>c</sub>     | 90                 | 7163                                     | 1885 | 3233   | 5874   | 10 401 | 16 519        | 211            | 1124                      | 1.50          | 83             | 3798                      | 1.66          | 35             | 924                       | 1.37     |
|                        | WL <sub>c</sub>     | 73                 | 5661                                     | 992  | 1659   | 3941   | 10 207 | 16 108        | 192            | 1413                      | 1.63          | 68             | 2275                      | 1.63          | 31             | 270                       | 1.37     |
|                        | CD <sub>c</sub>     | 70                 | 6629                                     | 1610 | 2594   | 5743   | 10 451 | 14 902        | 148            | 2247                      | 1.67          | 57             | 3479                      | 1.71          | –              | –                         | –        |
| Cruise                 | ES <sub>s</sub>     | 88                 | 5571                                     | 1450 | 2259   | 4618   | 8391   | 17 276        | 132            | 2123                      | 1.55          | 59             | 2484                      | 1.62          | –              | –                         | –        |

Title Page

Abstract

Introduction

Conclusions

References

Tables

Figures

◀

▶

◀

▶

Back

Close

Full Screen / Esc

Printer-friendly Version

Interactive Discussion



## Submicron aerosols at thirteen diversified sites in China

J. F. Peng et al.

Title Page

Abstract

Introduction

Conclusions

References

Tables

Figures



Back

Close

Full Screen / Esc

Printer-friendly Version

Interactive Discussion



**Table 3.** Summary of parameters of NPF events at different sites.

| Site            | Type       | Country  | Season     | CS ( $\times 10^{-2} \text{ s}^{-1}$ )* | GR ( $\text{nm h}^{-1}$ )* | Source                   |
|-----------------|------------|----------|------------|---|----------------------------|--------------------------|
| WX <sub>u</sub> | Urban      | China    | Summer     | 1.7 (0.9–2.8)                           | 10.4 (6.2–13.3)            | This study               |
|                 |            |          | Winter     | None                                    | None                       | This study               |
| SH <sub>u</sub> | Urban      | China    | Summer     | 2.0 (1.0–3.3)                           | 8.0 (4.2–12)               | This study               |
| GZ <sub>u</sub> | Urban      | China    | Autumn     | 3.9 (2.6–5.6)                           | 10.9 (7.3–18.1)            | This study               |
| JH <sub>u</sub> | Urban      | China    | Autumn     | None                                    | None                       | This study               |
| UR <sub>u</sub> | Urban      | China    | Spring     | 1.6 (1.0–2.6)                           | –                          | This study               |
| Beijing         | Urban      | China    | Whole year | 0.6–6.1                                 | 0.1–11.2                   | (Wu et al., 2007)        |
| Lanzhou         | Suburban   | China    | Summer     | 1.6 (0.9–2.4)                           | 4.4 (1.4–17.0)             | (Gao et al., 2011)       |
| Mexico City     | urban      | Mexico   | Spring     | –                                       | 0.5–9                      | (Dunn et al., 2004)      |
| Tecamac         | Suburban   | Mexico   | Spring     | –                                       | 15–40                      | (Iida et al., 2008)      |
| New Delhi       | Urban      | India    | Autumn     | 5–7                                     | 15.0 (11.6–18.1)           | (Monkkonen et al., 2005) |
| Budapest        | Urban      | Hungary  | Whole year | 1.2                                     | 7.2 (2.0–13.3)             | (Salma et al., 2011)     |
| Po Valley       | Urban      | Italy    | Whole year | 1.0 (0.4–1.8)                           | 6.8 (4.2–8.0)              | (Hamed et al., 2007)     |
| JX <sub>r</sub> | Regional   | China    | Summer     | 2.2 (1.1–4.1)                           | 13.6 (7.9–19.6)            | This study               |
|                 |            |          | Winter     | None                                    | None                       | This study               |
| YF <sub>r</sub> | Regional   | China    | Summer     | 2.7 (0.5–5.3)                           | 12.3 (8.6–21)              | This study               |
| HS <sub>r</sub> | Regional   | China    | Autumn     | None                                    | None                       | This study               |
| KP <sub>r</sub> | Regional   | China    | Autumn     | 2.5 (0.3–8.6)                           | 7.4 (3.2–13.5)             | This study               |
| Back-garden     | Regional   | China    | Summer     | 2.6 (2.3–3.3)                           | 12.1 (4.0–22.7)            | (Yue et al., 2013)       |
| Xinken          | Regional   | China    | Autumn     | –                                       | 8.3 (2.2–19.8)             | (Liu et al., 2008)       |
| K-pusztá        | rural      | Hungary  | Summer     | 0.5 (0.06–1.4)                          | 6.1 (2.2–14.4)             | (Yli-Juuti et al., 2009) |
| WL <sub>c</sub> | Coastal    | China    | Autumn     | 2.6                                     | 7.5                        | This study               |
| BG <sub>c</sub> | Coastal    | China    | Autumn     | 1.4 (1.0–1.8)                           | 4.5 (3.2–7.5)              | This study               |
| CD <sub>c</sub> | Coastal    | China    | Spring     | 2.0 (1.9–2.1)                           | 5.7 (4.5–6.8)              | This study               |
| ES <sub>s</sub> | Marine     | China    | Spring     | 0.9 (0.8–1.1)                           | 2.8 (1.6–3.9)              | This study               |
| Shangdianzi     | Background | China    | Whole year | 2                                       | 4.3 (0.3–14.5)             | (Shen et al., 2011)      |
| Yellow Sea      | Marine     | China    | Spring     | –                                       | 3.4                        | (Lin et al., 2007)       |
| Foresthill      | Remote     | American | Winter     | –                                       | 2–8                        | (Creamean et al., 2011)  |
| Hyytiala        | Forest     | Finland  | Whole year | 0.2 (0.04–0.8)                          | 3.0 (0.2–12)               | (Maso et al., 2005)      |

\* The values outside the bracket represent the average CS or GR; the values inside the bracket represent the maximum and minimum CS or GR; "none" means that there is no NPF events found in the whole measurement; "–" means that the GR value can not be calculated (only for the site of UR<sub>u</sub>), or there is no such information in the reference paper.

## Submicron aerosols at thirteen diversified sites in China

J. F. Peng et al.

**Table 4.** Summary of contribution of NPF events to potential CCN during the time between 14:00 to 17:00 LT in all measurements.

|          | Spring      |             | Summer      |             | Autumn      |             | Winter      |             |
|----------|-------------|-------------|-------------|-------------|-------------|-------------|-------------|-------------|
|          | $S_c = 0.5$ | $S_c = 0.2$ | $S_c = 0.5$ | $S_c = 0.2$ | $S_c = 0.5$ | $S_c = 0.2$ | $S_c = 0.5$ | $S_c = 0.2$ |
| Urban    | 33 %        | 6 %         | 66 %        | 26 %        | 31 %        | 9 %         | 0 %         | 0 %         |
| Regional | –           | –           | 57 %        | 23 %        | 30 %        | 6 %         | 0 %         | 0 %         |
| Coastal  | 10 %        | < 1 %       | 28 %        | 5 %         | 0 %         | 0 %         | –           | –           |
| Cruise   | < 1 %       | < 1 %       | –           | –           | 8 %         | < 1 %       | –           | –           |
|          |             |             |             |             | 5 %         | < 1 %       | –           | –           |
|          |             |             |             |             | –           | –           | –           | –           |

“–” represents that there is no measurement at that type of sites in the certain season; “0 %” represent that there is no NPF event found in the measurement; “< 1 %” represent that there are NPF events found in the measurement, but the relative contributions of these NPF events to the total CCN concentration are smaller than 1 %.

[Title Page](#)
[Abstract](#)
[Introduction](#)
[Conclusions](#)
[References](#)
[Tables](#)
[Figures](#)
[◀](#)
[▶](#)
[◀](#)
[▶](#)
[Back](#)
[Close](#)
[Full Screen / Esc](#)
[Printer-friendly Version](#)
[Interactive Discussion](#)


## Submicron aerosols at thirteen diversified sites in China

J. F. Peng et al.

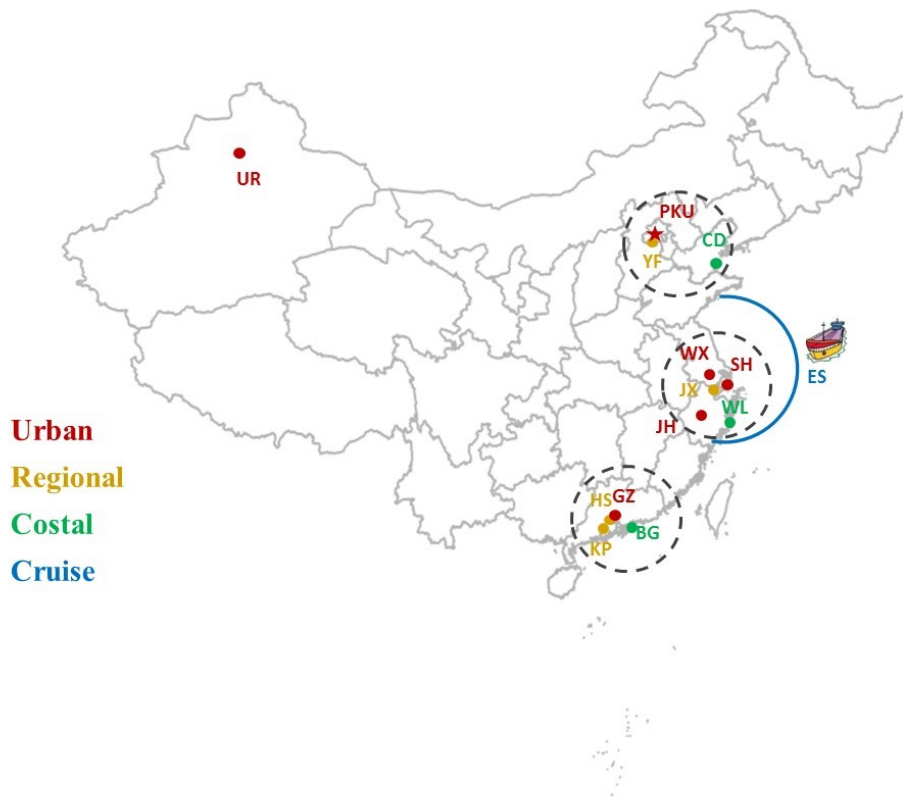


**Figure 1.** The location of all the thirteen measurement sites. Red, yellow, green and blue color dots represent the site type (urban, regional, costal and cruise. Black circles show the three largest urban areas in China.

Title Page

Abstract

Introduction

Conclusions

References

Tables

Figures



Back

Close

Full Screen / Esc

Printer-friendly Version

Interactive Discussion



**Submicron aerosols at thirteen diversified sites in China**

J. F. Peng et al.

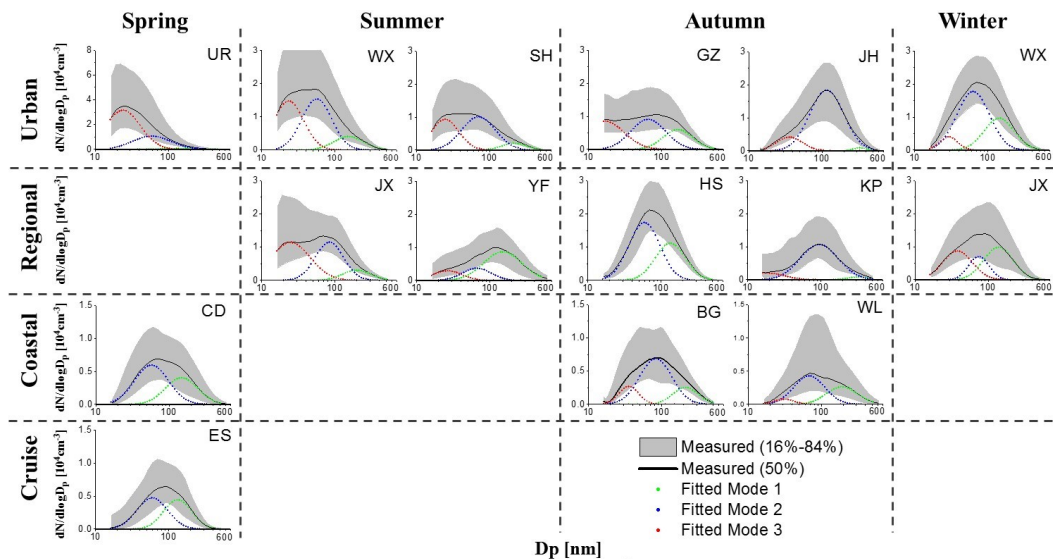


**Figure 2.** Median distribution (solid black line), 16th and 84th percentile distribution (shaded areas) and fitted mode (green, blue and red scatter dots) at all the measurement sites.

Title Page

Abstract

Introduction

Conclusions

References

Tables

Figures

◀

▶

◀

▶

Back

Close

Full Screen / Esc

Printer-friendly Version

Interactive Discussion



Submicron aerosols at thirteen diversified sites in China

J. F. Peng et al.

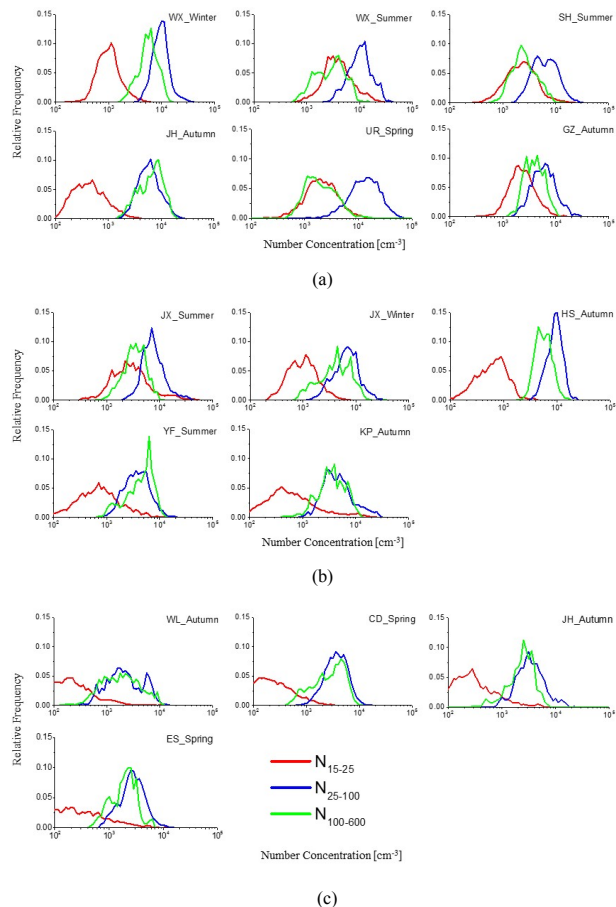


**Figure 3.** Distribution of PNC in different size ranges at (a) urban sites, (b) regional sites, (c) coastal sites and ship measurement. The red, blue and green line represents the distribution of  $N_{15-25}$ ,  $N_{25-100}$  and  $N_{100-600}$ , respectively.

Title Page

Abstract Introduction

Conclusions References

Tables Figures

◀ ▶

◀ ▶

Back Close

Full Screen / Esc

Printer-friendly Version

Interactive Discussion



## Submicron aerosols at thirteen diversified sites in China

J. F. Peng et al.

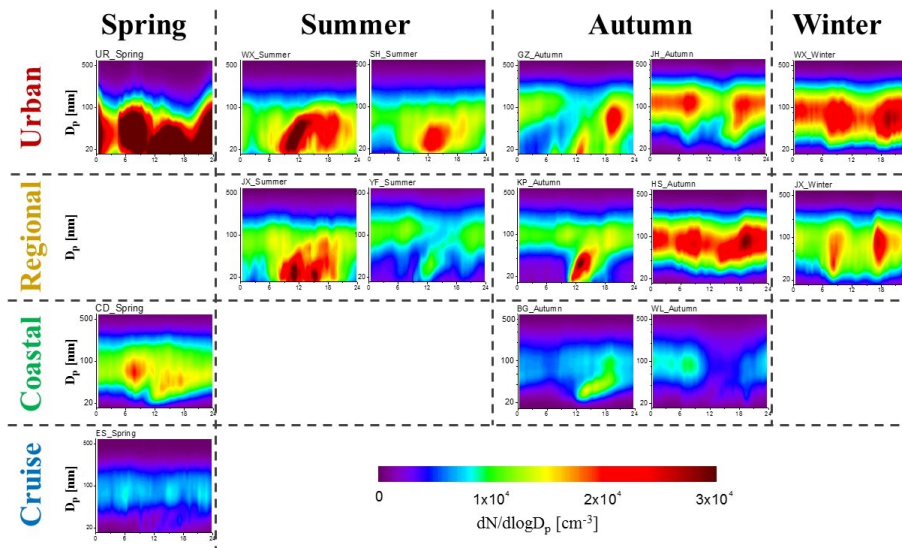


**Figure 4.** Diurnal variation of PNDs during measurements at different types of sites during different seasons. The color represents  $dN/d\log D_p$  ( $\text{cm}^{-3}$ ). All diurnal variation figures use the same axis and color bar.

[Title Page](#)
[Abstract](#)
[Introduction](#)
[Conclusions](#)
[References](#)
[Tables](#)
[Figures](#)
[◀](#)
[▶](#)
[◀](#)
[▶](#)
[Back](#)
[Close](#)
[Full Screen / Esc](#)
[Printer-friendly Version](#)
[Interactive Discussion](#)


**Submicron aerosols at thirteen diversified sites in China**

J. F. Peng et al.

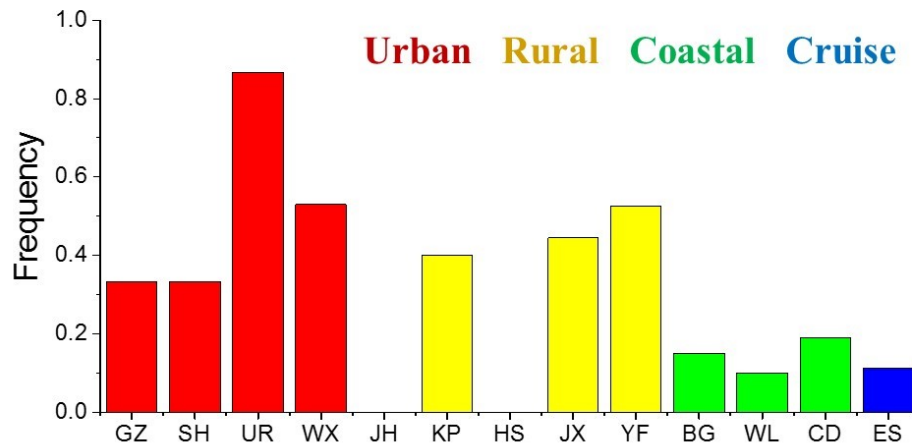


**Figure 5.** Frequencies of NPF events at different sites. The color of red, yellow, green and blue represent the site type of urban, rural, coastal and cruise, respectively.

[Title Page](#)[Abstract](#)[Introduction](#)[Conclusions](#)[References](#)[Tables](#)[Figures](#)[◀](#)[▶](#)[◀](#)[▶](#)[Back](#)[Close](#)[Full Screen / Esc](#)[Printer-friendly Version](#)[Interactive Discussion](#)



## Submicron aerosols at thirteen diversified sites in China

J. F. Peng et al.

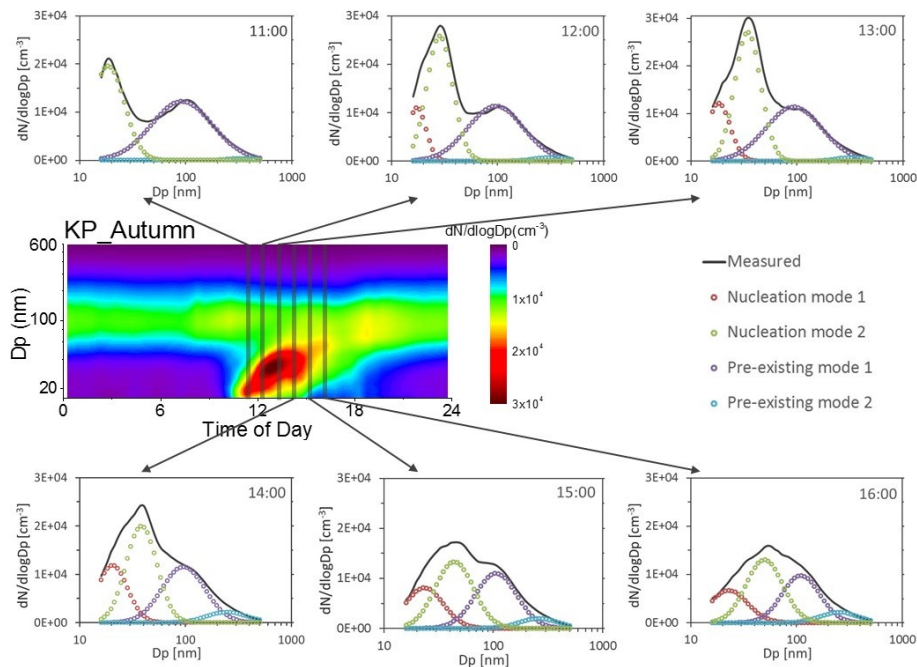


**Figure 6.** Lognormal fitting result of diurnal average PND at KP<sub>r</sub> site. The six line and symbol pictures show the mode fit results for the diurnal variation from 11:00 to 16:00 LT at KP site. Totally two nucleation modes and two pre-existing modes are found by mode fitting.